A Potential Peptide Inhibitor of SARS-CoV-2 S and human ACE2 Complex.

Grijesh Jaiswal
Amity University Noida
Veerendra Kumar (vkumar34@amity.edu)
Amity University Noida

Research Article

Keywords: SARS-CoV-2, COVID-19, peptide inhibitor, Immunoinformatic, receptor binding domain, spike S protein, angiotensin-converting enzyme 2 (ACE2)

Posted Date: October 7th, 2020

DOI: https://doi.org/10.21203/rs.3.rs-86815/v1

Version of Record: A version of this preprint was published at Journal of Biomolecular Structure and Dynamics on March 1st, 2021. See the published version at https://doi.org/10.1080/07391102.2021.1889665.

Abstract

The disease COVID-19 has caused heavy socio-economic burden and there is urgent need to control the SARS-CoV-2 (severe acute respiratory syndrome coronavirus 2) pandemic. The viral entry into human cell depends on the attachment of spike (S) protein to human cell receptor angiotensin-converting enzyme 2 (ACE2). We have designed a peptide inhibitor (ΔABP- α2) targeting the receptor binding domain (RBD) of S protein using *in silico* approach. Docking studies and computed affinities suggest peptide inhibitor binds at the RBD with 10-fold higher affinity than hACE2. MD simulation confirm the stable binding of inhibitor to hACE2. Immunoinformatic studies non-immunogenic nature of peptide. Thus, the proposed peptide could serve potential therapeutics for viral infection.

Introduction

The ongoing global pandemic COVID-19 is caused by a novel β-coronavirus SARS-CoV-2 (previously known as 2019-nCoV). The virus was first reported at the Wuhan (China) where the coronavirus caused an outbreak of pulmonary disease in late December 2019 [1,2]. SARS-CoV-2 is third coronavirus to cause substantial human disease after SARS-CoV and MERS-CoV. It transfers from human to human efficiently. Coronaviruses are positive-stranded RNA enveloped viruses. SARS-CoV-2 genome is about 82% identical to the SARS coronavirus (SARS-CoV) [3,4].

The S protein extensively decorates the virion surface as crown (therefore called corona). The spike (S) protein is type I membrane protein and glycosylated at 22 sites [5–8]. The S protein is analogous to influenza hemagglutinin (HA), respiratory syncytial virus (RSV) fusion glycoprotein (F), and human immunodeficiency virus (HIV) gp160 (Env). It facilitates the coronavirus entry into host cell [9,10]. The S protein consist of receptor binding S1 and membrane fusion S2 subunits. The S1 subunit consists of receptor binding domain (RBD) and core domain. The RBD consist of a receptor-binding motif (RBM), which interacts with the claw-like structure of ACE2 [11,12]. The S1 adopts elongated structure and undergoes transient hinge-like motions to become either receptor accessible or inaccessible. The monomeric form consists of consists of a large ectodomain, a single-pass transmembrane anchor, and a short intracellular tail at C-terminus 13,14.

The virus entry to human start with the attachment of S protein to the cell membrane protein receptor angiotensin-converting enzyme 2 (ACE2) [15,16]. The human ACE2 (hACE2) is expressed on the surface of alveolar cells of the lungs. Upon binding of ACE2, viral and host cell membranes fuse and the viral genome is injected into the host cell. The S protein is then cleaved into S1 and S2 subunits at furin-like cleavage site [17–19]. The RBD through its RBM site directly binds to the peptidase domain (PD) of h ACE2 [20,21]. The N-terminal α1 helix hACE2 engages with the RBM motif. Later, S1 subunit dissociates from ACE2 and S2 subunit adopts a post fusion state for membrane fusion [19–21]. The viral membrane and host cell membrane fuse to form a pore and viral genom is injected into host cell. This leads to the COVID-19 disease, which is associated with a major immune inflammatory response. Deaths are due to respiratory failure associated with cytokine storm with high serum levels of pro-inflammatory cytokines and chemokines [22].

SARS-CoV-2 spike (S) protein binds to hACE2 with higher affinity than the other SARS-CoV S proteins, a likely reason for SARS-CoV-2 high infectivity[23 5,24]. The monoclonal antibodies for SARS-CoV S protein are not able to neutralize SARS-CoV-2 [25]. Thus, despite the high sequence and structural similarity, there are notable differences between the SARS-CoV and SARS-CoV-2 S proteins. The affinity between the viral RBD and host ACE2 during the initial attachment of virus determines the susceptibility of hosts to the SARS-CoV infection [12,26,27]. Thus, viral entry into the host cell is a critical step in viral infection and could be exploited for therapeutics developments.

The current pandemic has created urgent needs for therapeutics or vaccines to treat COVID-19. Although scientist around the world are working to find a therapeutics or vaccines, till date, there are no clinically approved drugs to combat COVID-19. Computational approaches have been employed to discover the potential drugs against SARS-CoV-2 [28–32]. Drugs targeting either the S protein or proteases domain, have been screened. The inhibitors that can effectively block association of the SARS-CoV-2 S protein with hACE2 may have the potential to treat COVID-19. In our previous study, we have identified a double helical inhibitor ΔABP-D25Y (residue 65) that binds at the RBM site of SARS-CoV-2 RBD with higher affinity than hACE2. To further improve the potency of identified inhibitor and minimize the immunogenicity, we have found out a 28 aa long peptide which binds RBD with 10-fold higher affinity than ΔABP-D25Y.

Materials And Methods

Structural analysis:

All the protein structures were downloaded from Protein Data Bank (PDB) and their codes are mention as they appear in the manuscript [33]. The structures were manually visualised and manipulated in Coot, Pymol and UCSF Chimera [34–36]. Structural comparison was done using Pymol. Multiple sequence alignment was done using Clustal omega server [37]. All the figures were prepare using Pymol [35]. Binding affinity was computed using PRODIGY server [38].

Molecular docking:

Molecular docking is used to dock the binding of a peptide or ligand on a macromolecule. The RBD domain (336-518) of SARS-CoV-2 S protein (PDB 6M17) was used as a receptor molecule. The ΔABP- α1 (LKYLVKQLERALRELKKSLDELERSLEELEKN), ΔABP- α1-V10K (LKYLKKQLERALRELKKSLDELERSLEELEKN), ΔABP- α1-D25Y (LKYLVKQLERALRELKKSLYELERSLEELEKN), ΔABP- α1-V10K-D25Y (LKYLKKQLERALRELKKSLYELERSLEELEKN), and ΔABP- α2 (PSEDALVENNRLNVENNKIIVEVLRIIL) peptides were docked using HADDOCK2.4 program [39]. Docking by HADDOCK program is driven by prediction of likely residues (called ambiguous interaction restraints (AIRs)) found at the interface. These residues may be active (interacting residue) or passive (nearby interacting residue). Binding interface of RBD and peptides were predicted using CPORT [40] and BIPSPI [41] servers. Before docking protocol, the pdbs were “cleaned” by removing water and non-bonded ions.

Molecular Dynamics (MD) Simulations:

The MD simulation was performed for RBD (residues 336-518) and ΔABP- α2 complex in Gromacs 2020.2 for 100 ns [42]. Simulation inputs were built using CHARMM-GUI web with CHARMM36 force field [43,44]. The complex was immersed in a cubic box filled with TIP3P water molecules and 150 mM NaCl. The sodium and chloride ions were added to neutralize the charge of the system. All simulations were run using Periodic Boundary Conditions (PBC). Initial geometries of the system were minimised with 5,000 steps with the steepest descent algorithm. The system was relaxed at 303 K and 1 atm for 500 ps at 2 fs time steps. Production MD was performed for 100 ns. During production run temperature was maintained at 303 K using velocity rescaling. Bond lengths were constrained with the LINCS algorithm. The pressure was controlled by isotropic coupling using Parrinello-Rahman barostat. A Verlet scheme was used for van der Waals and Particle Mesh Ewald electrostatics interactions within 1.2 nm. Van der Waals interactions were switched above 1.0 nm.

Principal Component Analysis (PCA):

PCA was done to detect the direction and amplitude of the dominant motions in the MD trajectory [45]. PCA method is used reduces the complexity of a data set to extract biologically relevant movements of protein domains. GROMACS in built tool covar was used to obtain eigenvalues and eigenvectors by calculating and diagonalizing the covariance matrix. This removed the translational and rotational components from the system. The eigenvectors that correspond to the largest eigenvalues are called principal components (PCs). They represent the largest-amplitude collective motions. GROMACS utility tool anaeig was used to analyse the eigenvectors.

Immunoinformatic:

The protective antigens were predicted from VaxiJen 2.0 with default parameters [46]. The T-cell epitopes were identified using NetCTL 1.2 server which outputs the combinatorial score of MHC-I binding, proteasomal C-terminal cleavage, and TAP transport [47]. B cell epitope prediction was done using IEDB tool. DiscoTope tool was used conformational B cell epitope prediction [48].

Results

Several SARS-CoV-2 RBD and hACE2 complex structures have been solved and deposited in Protein Data Bank (PDB). We use pdb 6M17 for our analysis. The peptide inhibitor is derived from ABP (pdb code 6H9H) as described in our previous studies[49].

Docking analysis:

The previously identified inhibitor (ΔABP-D25Y) of RBD has two helices (α1 and α2) homologous to PD domain of hACE2 [49]. The inhibitor (ΔABP-D25Y) binds to RBD with higher affinity compared to hACE2. To further examine the role of individual helices of ΔABP in interaction with RBD, we examined following peptides - ΔABP-α1, ΔABP- α2, ΔABP- α1-V10K, ΔABP-α1-D25Y, and ΔABP-α1-V10K- D25Y. The mutations

(D25Y and V10K) were introduced to complement the α1 helix of hACE2[49]. We docked all peptides into SARS-CoV-2 RBD. The interaction restraints were generated using CPORT and BIPSPI servers [40,41]. Both servers predicted peptides binding at RBM site of RBD. Therefore, RBM site residues (483-507) and all residues of peptides were used as active residues for docking. Best complex structures were selected based on cluster size and HADDOCK score. HADDOCK score is computed as a weighted sum of van de Waals, electrostatic, desolvation, and ambiguous interaction restraints energies. The ΔABP-α2 showed the best HADDOCK score (Table 1). ΔABP-α2 peptide sits between the two helices of ΔABP-D25Y (Fig 1A and Supplementary file 1). The N terminus and C-terminus of peptide are shifted about 8.9 Å and 3.2 Å respectively, towards RBD in comparison to α2 helix ofΔABP-D25Y. Thus, the ΔABP-α2 is closer to RBD compared to ΔABP-D25Y. The ΔABP-α2 peptide partially overlap with α1 helix of hACE2 (Fig 1B). The fragment up to residue Ile56 (His34 of hACE2) superimpose very well. From residue Glu35 (hACE2) onwards the α1/hACE2 deviates away from SARS-CoV-2 RBD. However, ΔABP-α2 peptide lies parallel to RBM throughout its length (Fig 1B). Hence the bound peptide showed higher binding affinity for SARS-CoV-2 RBD.

However, the ΔABP-α1 peptide and its mutants bind SARS-CoV-2 RBD with lower affinity (Table 1). Further, the ΔABP-α1 peptides bind at a different position than the α1 helix of ΔABP-D25Y (Supplementary Fig 1A). The ΔABP-α2 peptide also binds RBD of other coronaviruses at the same site. Binding score varies depending on the RBM site residues. The ΔABP- α2 peptide binds 2005-2006 SARS coronavirus civet strain RBD (pdb 3d0i) with best HADDOCK score (-85.6 +/- 0.2). The binding score is better than SARS-CoV-2 RBD. However, the bound peptide does not cover the whole RBM site (Supplementary Fig 1B). Thus, the proposed inhibitor has the potential to block the broader range of coronaviruses.

Binding affinity:

The binding affinity of the therapeutic agents to the receptor is an important parameter in predicting their effectiveness as promising drug candidates. To compute the binding affinity of peptides, we use PRODIGY server. The binding affinities of induvial peptides are listed in table 1. The predicted affinities are in accordance with HADDOCK score. The PRODIGY server predicted a dissociation constant (K_D) of 2.6 nM (ΔG -11.7 kcal mol^{-1}) and 0.049 nM (ΔG -14.1 kcal mol^{-1}) for ΔABP- α1 and ΔABP- α2 peptides, respectively. The predicted K_D of ΔABP-D25Y is 0.6 nM (ΔG -12.6 kcal mol^{-1}) [49]. The dissociation constants of mutant ΔABP- α1-V10K, ΔABP- α1-D25Y, and ΔABP- α1-V10K-D25Y are 16.0 nM (ΔG -10.6 kcal mol^{-1}), 5.2 nM (ΔG -11.3 kcal $mol^{-}1$), and 69 nM (ΔG -9.8 kcal mol-1) respectively. The order of peptides affinity to SARs-CoV-2 RBD is ΔABP- α2 > ΔABP- α1 > ΔABP-D25Y > ΔABP- α1-D25Y > ΔABP- α1-V10K > ΔABP- α1-V10K-D25Y. The experimentally determined K_D for hACE2 to ectodomain S protein interaction is 4.7 nM [5,24]. Thus, ΔABP- α2 peptide binds SARS-CoV-2 RBD with higher affinity than hACE2. A designed inhibitor should have a selective binding at the target site with relatively high binding energies. Thus, HADDOCK score and predicted K_D suggests that ΔABP-α2 peptide binds RBD with remarkably high affinity.

ΔABP-α2 Complex:

The peptide ΔABP-α2 is parallelly aligned with RBM β sheet and covers the whole RBM site (Fig 1). The N-terminus of peptide interacts with the RBD capping loop (472-488) and C-terminus of peptide interacts with RBD loop (498-505). Thus, ΔABP-α2 peptide forms extensive contact with SARS-CoV-2 RBD. Sequence analysis of coronaviruses RBDs suggest that SARS-CoV-2 RBD has unique residues- Leu455, Phe486, Gln493, Ser494, and Asn501. These unique residues form extensive contact with hACE2 and responsible for higher affinity of SARS-CoV-2 RBD to hACE2[20,21,50]. Thus, the designed inhibitor should disengage these residues from hACE2 interaction.

Leu455 of SARS-CoV-2 RBD enhances the viral binding to hACE2 because of its favourable interactions with hotspot 31 (Lys31 of hACE2)[10]. In SARS-CoV-2 RBD, Leu455 interacts with Asp30, Lys31, and His34 of hACE2. In RBD/ΔABP-α2 peptide complex, Leu455 interacts with GLU52, ASN53, Lys55, and ILE56 (Fig 2A). In SARS-CoV-2 RBD, Phe486 does not interact with α1/hACE2. Capping loops which harbours Phe486 is flexible and deviates towards bound peptide in ΔABP-α2 complex. In ΔABP-α2, Phe486 is coordinated by triad Leu43, Asn46, Asn47. The phenyl ring of Phe486 is sandwiched between side chain of Asn46 and Asn47 (Fig 2B). In SARS-CoV-2 RBD, Gln493 forms salt bridge interactions with Lys31 and Glu35 of hACE2. In ΔABP-α2/RBD complex also, Gln493 forms similar strong salt bridge interaction with ASN53 of peptide (Fig 2C). Ser494 does not involve in any interaction in SARS-CoV-2 RBD and hACE2 complex. However, in ΔABP-α2 complex Ser494 forms interaction with Val60 of ΔABP-α2 enhancing peptide interaction with viral RBD (Fig 2C). Lastly, Asn501 in SARS-CoV-2 RBD/hACE2 complex interacts with Tyr41 of ACE2. However, Asn501 interacts with Arg62 and Ile63 of peptide in. ΔABP-α2 (Fig 2D). Thus ΔABP-α2 can from the very strong interaction with RBD.

MD Simulation:

To understand the interactions between viral RBD and ΔABP-α2 100 ns classical MD simulation of the complex was performed. To assess the dynamic behaviour of the complex, the time dependent root-mean-square deviation (RMSD) of all protein atoms was calculated using original docked complex as reference. The RMSD value of the whole complex fluctuates between 0.3-0.4 nm suggesting flexible nature of the complex (Fig 3A). Both the RBM site and ΔABP-α2 peptide exhibit RMSD value of ~0.2 nm. Thus, the interface between peptide inhibitor and RBM is stable (Fig 3A).

The dynamic behaviour of protein at residue level was estimated by root-mean-square fluctuations (RMSF) calculation (Fig 3B). RMSF reflects the positions of the individual atoms with respect to the average position across the whole simulation trajectory. The peptide ΔABP-α2 residues are rigid and does not fluctuate much (RMSF < 0.15 Å) (Fig 3B). Similarly, the RBD residues are stable except some loops. Particularly two flexible regions are present in the RBD. The loop between (380-396) on the surface of RBD is flexible. This loop is far from the hACE2 interaction site. The second flexible region is the capping loop (476-490) near the hACE2 interaction site. The composition of this loop is remarkably different from SARS-COV. The following mutations Pro469/Val483, Pro470/Glu484, Thr468/Gly482, Cys467/Cys480, Lys465/Thr478, Asp463/Gly476, Pro462/Ala475 (SARS-CoV/SARS-CoV-2) makes SARS-CoV-2 loop more flexible. An extra amino acid Asn481 in SARS-CoV-2 loop is present. The absence of two Pro residues, presence of Gly and Cys, and insertion of Asn481 in SARS-CoV-2 make the capping loop more flexible (RMSF ~ 0.8 nm) (Fig 3B).

However, interface residues showed overall low RMSF (0.1-0.2 nm) and all critical amino acids maintain their interactions with ΔABP-α2 peptide. The single α helical peptide inhibitor of SARS-CoV-2 based on PD domain of hACE2 was found to be less stable[51]. However, ΔABP-α2 peptide retain its shape and provide full coverage to the RBM site (Fig 3B).

Radius of gyration (Rg) is the measure the compactness of the molecule in the solution. The Rg SARS-CoV-2 RBD and ΔABP-α2 peptide complex fluctuates between 1.87-1.97 nm. Significant variation is seen at around 50 ns simulation which can be attributed to the flexible loops of RBD (Fig 3C). Similarly, solvent accessible surface area (SASA) curve supports the Rg plot (Fig 3D). Thus, classical MD simulation studies suggest that the interface of the complex is stable, and the inhibitor ΔABP-α2 does not dissociate from RBD. A good peptide inhibitor should have selective binding to the receptor, complementary shape, and low flexibility of the interface residues [52].

Principle component analysis (PCA):

PCA is a standard method to characterize the variable correlations from atomic fluctuations in an MD trajectory. PCA can provide a brief description of the motions. PCA extracts highly correlated motions from MD trajectories using dimensional reductions. To understand the motion of ΔABP-α2 peptide, RBM site, and capping loop, PCA analysis was performed (Fig 4). The core of the RBD, the bound peptide, and RBM site do not show any motion (Fig 4A). The C terminus of peptide showed slight twisting motion and shifted away from RBD significantly (~ 6.0 Å). These residues are not involved in direct interaction with RBD. Without complete protein fold, the isolated helical peptides are usually unstable which in turn reduces the affinity of the peptides to the target protein[53]. The peptide ΔABP-α2 maintained its helicity and remained bound to viral RBD throughout the simulations. The pose of peptide did not change during the simulation. Specially, the central portion of peptide ΔABP-α2 maintains its interaction with viral RBD (Supplementary file 2).

However, the capping loop (476-490) of the peptide showed highest degree of motion (Fig 4B). The fluctuates between open and close conformations (Fig 4B and Supplementary File 2). The ΔABP-α2 peptide maintains its interaction with capping throughout its transition from open to closed state. The second significant motion occurs in the fragment between residues (358-394) of RBD. This region is on the surface of RBD and far from the interface of RDM and ΔABP-α2 peptide (Fig 4C).

Immunoinformatics:

The peptide inhibitor is recognised as a foreign substance by the human host cells, thus inducing a host immune response[54]. The antibodies can affect the efficacy of the drug by reducing the lifetime, neutralising the activity, and altering the pharmacokinetics of the drug. Thus, an ideal inhibitor should not be antigenic. The ΔABP-α2 peptide was not antigenic according to VaxiJen 2.0 server [46]. The server predicted protective antigen score of -0.0046, which is much lower than the threshold 0.4. The B cell epitope is a portion of an antigen recognized by either a particular B cell receptor or the elicited antibody [55]. There are two types of B cell epitopes -1) Continuous and linear and 2) Discontinuous or structural. More than 90% of B cell epitopes

are structural [56–58]. DiscoTope analysis suggests the propensity scores of the individual residues for discontinuous B cell epitope (Fig 5A).

The recognition of viral peptides-MHC class I complex by $CD8^+$ T cells is necessary for antiviral immunity. The T cell epitopes are necessary to design an effective vaccine, however, will pose a challenge for peptide-based drugs. We used NetCTL 1.2 server to predict Cytotoxic T lymphocyte (CTL) epitopes (Fig 5B). This tool outcomes combined score of MHC class I binding, proteasomal C terminal cleavage and TAP transport efficiency. The highest score (0.5391) was seen for peptide (LVENNRLNV). Thus, no CTL epitopes were predicted on ΔABP-α2 sequence. Thus, above analysis suggest the ΔABP-α2 is non immunogenic and will be a probable candidate for therapeutic use.

Discussion

The COVID-19 pandemic has caused the inconceivable loss to the economy and human lives. As of now, no specific prophylactic or postexposure medicine is available to treat COVID-19. The vaccines have been proved to be the most powerful tool to fight the viral infections. However, traditional drug discovery is not an efficient option as this process takes long time. Different strategies have been employed to develop therapeutics to combat the SARS-CoV-2 [59–63]. The molecules that can effectively check the interaction of SARS-CoV-2 S protein with hACE2 will be a potential drug candidate. In this study, we have reported a synthetic protein molecule ΔABP-α2 which have the potential to block the association of viral S protein with hACE2.

Peptides are smaller and easy to produce either chemically or biologically. The advantages of peptides as drugs includes the low toxicity, ease of modifications, specificity to the target, greater affinity etc. Huang et al[64] have proposed a peptide inhibitor for SARS-CoV-2 and hACE2 association using EvoDesign approach. The proposed inhibitor showed a stronger binding affinity to RBD compared to hACE2[64]. Hsiang et el have showed that the peptides SP-4 (GFLYVYKGYQPI), SP-8 (FYTTTGIGYQPY) and SP-10 (STSQKSIVAYTM) can significantly block the interaction of SARS-CoV S protein with hACE2[65]. However, these peptides are derived from viral spike protein and their target is hACE2. This will limit their use as therapeutics because they might affect normal function of hACE2[65]. Baig et all used alanine scanning method to design a peptide inhibitor against SARA-CoV-2 RBD [50]. Han and Kral also showed potential peptide inhibitors of RBD derived from PD domain of hACE2[51]

One critical limitation in using peptide inhibitors as drug is short half-life *in vivo*. However, the conjugation of peptides with lipid exhibit significantly improved antiviral potency and better pharmacokinetics[66,67]. The field of peptidomimetics is used to get derivatives of peptides which have better bioavailability, improved blood-brain barrier transport, reduced rate of clearance, and better stability against peptidases[68,69]. Some examples of peptidomimetics are the D-amino acid substitutes, altered amide bonds, peptoids, urea peptidomimetics, peptide sulfonamides, oligocarbamates, partial or full retro-inverso peptides, azapeptides, β-peptides and N-modified peptides etc. Further, computational protein design can be combined with experimental setup to accelerate the drug design. We have verified the binding of ΔABP-α2 peptide to SARS-

CoV-2 RBD by various computations tools. However, it warrants the experimental verification to assess the drug ability of ΔABP-α2.

Conclusion

In summary, using classical MD simulations, we have shown that peptide ΔABP-α2 extracted from ABP provide highly promising trail for SARS-CoV-2 blocking. MD simulations revealed that peptides maintain their helical structure and provide a highly specific and stable binding to SARS-CoV-2 RBD. The ΔABP-α2 peptide specifically engages with critical residues of SARS-CoV-2 RBD. Binding affinity prediction suggests the peptide binds to viral RBD with 10-fold higher affinity than hACE2. Thus, peptide will outcompete the hACE2. Immunoinformatics analysis suggest that proposed peptide inhibitor is non-immunogenic for both B and T cells.

Declarations

Author Contributions:

Conceived and designed the experiments: VK. Performed the experiments: GJ and VK. Analysed the data: GJ and VK. Contributed to the writing of the manuscript: VK

Conflict of interest: The authors declare no competing financial interest.

Acknowledgement:

We would like to acknowledge the Ramalingaswami Fellowship (BT/RLF/Re-entry/64/2017), Department of Biotechnology, Govt of India (VK). The funders had no role in study design, data collection and analysis, decision to publish, or preparation of the manuscript.

References

1. Zhou, P. *et al.* A pneumonia outbreak associated with a new coronavirus of probable bat origin. *Nature* (2020) doi:10.1038/s41586-020-2012-7.
2. Wu, F. *et al.* A new coronavirus associated with human respiratory disease in China. *Nature* **579**, 265–269 (2020).
3. Ren, L. L. *et al.* Identification of a novel coronavirus causing severe pneumonia in human: a descriptive study. *Chinese medical journal* (2020) doi:10.1097/CM9.0000000000000722.
4. Zhu, N. *et al.* A novel coronavirus from patients with pneumonia in China, 2019. *New England Journal of Medicine* **382**, 727–733 (2020).
5. Walls, A. C. *et al.* Structure, Function, and Antigenicity of the SARS-CoV-2 Spike Glycoprotein. *Cell* (2020) doi:10.1016/j.cell.2020.02.058.
6. Simmons, G. *et al.* Characterization of severe acute respiratory syndrome-associated coronavirus (SARS-CoV) spike glycoprotein-mediated viral entry. *Proceedings of the National Academy of Sciences*

of the United States of America (2004) doi:10.1073/pnas.0306446101.

7. Kumar, S., Maurya, V. K., Prasad, A. K., Bhatt, M. L. B. & Saxena, S. K. Structural, glycosylation and antigenic variation between 2019 novel coronavirus (2019-nCoV) and SARS coronavirus (SARS-CoV). *VirusDisease* (2020) doi:10.1007/s13337-020-00571-5.
8. Walls, A. C. *et al.* Glycan shield and epitope masking of a coronavirus spike protein observed by cryo-electron microscopy. *Nature Structural and Molecular Biology* (2016) doi:10.1038/nsmb.3293.
9. Li, F. Structure, Function, and Evolution of Coronavirus Spike Proteins. *Annual Review of Virology* (2016) doi:10.1146/annurev-virology-110615-042301.
10. Wan, Y., Shang, J., Graham, R., Baric, R. S. & Li, F. Receptor Recognition by the Novel Coronavirus from Wuhan: an Analysis Based on Decade-Long Structural Studies of SARS Coronavirus. *Journal of Virology* (2020) doi:10.1128/jvi.00127-20.
11. Li, F., Li, W., Farzan, M. & Harrison, S. C. Structural biology: Structure of SARS coronavirus spike receptor-binding domain complexed with receptor. *Science* (2005) doi:10.1126/science.1116480.
12. Li, W. *et al.* Efficient Replication of Severe Acute Respiratory Syndrome Coronavirus in Mouse Cells Is Limited by Murine Angiotensin-Converting Enzyme 2. *Journal of Virology* (2004) doi:10.1128/jvi.78.20.11429-11433.2004.
13. Bosch, B. J., van der Zee, R., de Haan, C. A. M. & Rottier, P. J. M. The Coronavirus Spike Protein Is a Class I Virus Fusion Protein: Structural and Functional Characterization of the Fusion Core Complex. *Journal of Virology* (2003) doi:10.1128/jvi.77.16.8801-8811.2003.
14. Gao, J. *et al.* Structure of the Fusion Core and Inhibition of Fusion by a Heptad Repeat Peptide Derived from the S Protein of Middle East Respiratory Syndrome Coronavirus. *Journal of Virology* (2013) doi:10.1128/jvi.02433-13.
15. Li, W. *et al.* Angiotensin-converting enzyme 2 is a functional receptor for the SARS coronavirus. *Nature* (2003) doi:10.1038/nature02145.
16. Tai, W. *et al.* Characterization of the receptor-binding domain (RBD) of 2019 novel coronavirus: implication for development of RBD protein as a viral attachment inhibitor and vaccine. *Cellular and Molecular Immunology* (2020) doi:10.1038/s41423-020-0400-4.
17. Hoffmann, M., Kleine-Weber, H. & Pöhlmann, S. A Multibasic Cleavage Site in the Spike Protein of SARS-CoV-2 Is Essential for Infection of Human Lung Cells. *Molecular Cell* (2020) doi:10.1016/j.molcel.2020.04.022.
18. Xia, S. *et al.* Fusion mechanism of 2019-nCoV and fusion inhibitors targeting HR1 domain in spike protein. *Cellular and Molecular Immunology* (2020) doi:10.1038/s41423-020-0374-2.
19. Coutard, B. *et al.* The spike glycoprotein of the new coronavirus 2019-nCoV contains a furin-like cleavage site absent in CoV of the same clade. *Antiviral Research* (2020) doi:10.1016/j.antiviral.2020.104742.
20. Yan, R. *et al.* Structural basis for the recognition of SARS-CoV-2 by full-length human ACE2. *Science* (2020) doi:10.1126/science.abb2762.

21. Shang, J. *et al.* Structural basis of receptor recognition by SARS-CoV-2. *Nature* (2020) doi:10.1038/s41586-020-2179-y.
22. Feldmann, M. *et al.* Trials of anti-tumour necrosis factor therapy for COVID-19 are urgently needed. *The Lancet* (2020) doi:10.1016/S0140-6736(20)30858-8.
23. Wrapp, D. *et al.* Cryo-EM structure of the 2019-nCoV spike in the prefusion conformation. *Science* (2020) doi:10.1126/science.aax0902.
24. Lan, J. *et al.* Structure of the SARS-CoV-2 spike receptor-binding domain bound to the ACE2 receptor. *Nature* (2020) doi:10.1038/s41586-020-2180-5.
25. Tian, X. *et al.* Potent binding of 2019 novel coronavirus spike protein by a SARS coronavirus-specific human monoclonal antibody. *Emerging Microbes and Infections* (2020) doi:10.1080/22221751.2020.1729069.
26. Li, F. Receptor Recognition Mechanisms of Coronaviruses: a Decade of Structural Studies. *Journal of Virology* (2015) doi:10.1128/jvi.02615-14.
27. Belouzard, S., Millet, J. K., Licitra, B. N. & Whittaker, G. R. Mechanisms of coronavirus cell entry mediated by the viral spike protein. *Viruses* (2012) doi:10.3390/v4061011.
28. Wu, C. *et al.* Analysis of therapeutic targets for SARS-CoV-2 and discovery of potential drugs by computational methods. *Acta Pharmaceutica Sinica B* (2020) doi:10.1016/j.apsb.2020.02.008.
29. Mirza, M. U.; Froeyen, M. Structural Elucidation of SARS-CoV-2 Vital Proteins: Computational Methods Reveal Potential Drug Candidates Against Main Protease, Nsp12 RNA-dependent RNA Polymerase and Nsp13 Helicase. *Preprints* (2020) doi:10.20944/preprints202003.0085.v1.
30. Khan, R. J. *et al.* Targeting SARS-CoV-2: A Systematic Drug Repurposing Approach to Identify Promising Inhibitors Against 3C-like Proteinase and 2'-O-RiboseMethyltransferase. *Journal of biomolecular structure & dynamics* (2020) doi:10.1080/07391102.2020.1753577.
31. Zhou, Y. *et al.* Network-based drug repurposing for novel coronavirus 2019-nCoV/SARS-CoV-2. *Cell Discovery* (2020) doi:10.1038/s41421-020-0153-3.
32. Chandel, V., Raj, S., Rathi, B. & Kumar, D. In silico identification of potent FDA approved drugs against Coronavirus COVID-19 main protease: A drug repurposing approach. *Chemical Biology Letters* (2020).
33. Berman, H. M. *et al.* The Protein Data Bank (www.rcsb.org). *Nucleic Acids Research* (2000) doi:10.1093/nar/28.1.235.
34. Waterhouse, A. *et al.* UCSF Chimera–a visualization system for exploratory research and analysis. *The Journal of biological chemistry* (2009) doi:10.1097/MLR.0000000000000625.
35. DeLano, W. L. The PyMOL Molecular Graphics System, Version 1.1. *Schr{ö}dinger LLC* (2002) doi:10.1038/hr.2014.17.
36. Emsley, P., Lohkamp, B., Scott, W. G. & Cowtan, K. Features and development of Coot. *Acta Crystallographica Section D: Biological Crystallography* (2010) doi:10.1107/S0907444910007493.
37. Sievers, F. *et al.* Fast, scalable generation of high-quality protein multiple sequence alignments using Clustal Omega. *Molecular Systems Biology* (2011) doi:10.1038/msb.2011.75.

38. Xue, L. C., Rodrigues, J. P., Kastritis, P. L., Bonvin, A. M. & Vangone, A. PRODIGY: A web server for predicting the binding affinity of protein-protein complexes. *Bioinformatics* (2016) doi:10.1093/bioinformatics/btw514.
39. van Zundert, G. C. P. *et al.* The HADDOCK2.2 Web Server: User-Friendly Integrative Modeling of Biomolecular Complexes. *Journal of Molecular Biology* (2016) doi:10.1016/j.jmb.2015.09.014.
40. de Vries, S. J. & Bonvin, A. M. J. J. Cport: A consensus interface predictor and its performance in prediction-driven docking with HADDOCK. *PLoS ONE* (2011) doi:10.1371/journal.pone.0017695.
41. Sanchez-Garcia, R., Sorzano, C. O. S., Carazo, J. M. & Segura, J. BIPSPI: A method for the prediction of partner-specific protein-protein interfaces. *Bioinformatics* (2019) doi:10.1093/bioinformatics/bty647.
42. Abraham, M. J. *et al.* Gromacs: High performance molecular simulations through multi-level parallelism from laptops to supercomputers. *SoftwareX* (2015) doi:10.1016/j.softx.2015.06.001.
43. Jo, S., Kim, T., Iyer, V. G. & Im, W. CHARMM-GUI: A web-based graphical user interface for CHARMM. *Journal of Computational Chemistry* (2008) doi:10.1002/jcc.20945.
44. Lee, J. *et al.* CHARMM-GUI Input Generator for NAMD, GROMACS, AMBER, OpenMM, and CHARMM/OpenMM Simulations Using the CHARMM36 Additive Force Field. *Journal of Chemical Theory and Computation* **12**, 405–413 (2016).
45. Yang, L. W., Eyal, E., Bahar, I. & Kitao, A. Principal component analysis of native ensembles of biomolecular structures (PCA_NEST): Insights into functional dynamics. *Bioinformatics* (2009) doi:10.1093/bioinformatics/btp023.
46. Doytchinova, I. A. & Flower, D. R. VaxiJen: A server for prediction of protective antigens, tumour antigens and subunit vaccines. *BMC Bioinformatics* (2007) doi:10.1186/1471-2105-8-4.
47. Larsen, M. v. *et al.* Large-scale validation of methods for cytotoxic T-lymphocyte epitope prediction. *BMC Bioinformatics* (2007) doi:10.1186/1471-2105-8-424.
48. Kringelum, J. V., Lundegaard, C., Lund, O. & Nielsen, M. Reliable B Cell Epitope Predictions: Impacts of Method Development and Improved Benchmarking. *PLoS Computational Biology* (2012) doi:10.1371/journal.pcbi.1002829.
49. Grijesh Jaiswal, V. K. In-silico Design of a Potential Inhibitor of SARS-CoV-2 S Protein. *PLoS ONE* **Accepted**, (2020).
50. Baig, M. S., Alagumuthu, M., Rajpoot, S. & Saqib, U. Identification of a Potential Peptide Inhibitor of SARS-CoV-2 Targeting its Entry into the Host Cells. *Drugs in R and D* (2020) doi:10.1007/s40268-020-00312-5.
51. Han, Y. & Král, P. Computational Design of ACE2-Based Peptide Inhibitors of SARS-CoV-2. *ACS Nano* (2020) doi:10.1021/acsnano.0c02857.
52. Wójcik, P. & Berlicki, Ł. Peptide-based inhibitors of protein-protein interactions. *Bioorganic and Medicinal Chemistry Letters* (2016) doi:10.1016/j.bmcl.2015.12.084.
53. Chakrabartty, A., Kortemme, T. & Baldwin, R. L. Helix propensities of the amino acids measured in alanine-based peptides without helix-stabilizing side-chain interactions. *Protein Science* (1994) doi:10.1002/pro.5560030514.

54. Fernandez, L. *et al.* Immunogenicity in Protein and Peptide Based-Therapeutics: An Overview. *Current Protein & Peptide Science* (2017) doi:10.2174/1389203718666170828123449.
55. Parker, D. C. T Cell-Dependent B Cell Activation. in *Encyclopedia of Immunobiology* (2016). doi:10.1016/B978-0-12-374279-7.09010-X.
56. Sanchez-Trincado, J. L., Gomez-Perosanz, M. & Reche, P. A. Fundamentals and Methods for T- and B-Cell Epitope Prediction. *Journal of Immunology Research* (2017) doi:10.1155/2017/2680160.
57. Potocnakova, L., Bhide, M. & Pulzova, L. B. An Introduction to B-Cell Epitope Mapping and in Silico Epitope Prediction. *Journal of Immunology Research* (2016) doi:10.1155/2016/6760830.
58. El-Manzalawy, Y. & Honavar, V. Recent advances in B-cell epitope prediction methods. *Immunome Research* (2010) doi:10.1186/1745-7580-6-S2-S2.
59. Zhou, Z. *et al.* A recombinant baculovirus-expressed S glycoprotein vaccine elicits high titers of SARS-associated coronavirus (SARS-CoV) neutralizing antibodies in mice. *Vaccine* (2006) doi:10.1016/j.vaccine.2006.01.059.
60. Dong, L., Hu, S. & Gao, J. Discovering drugs to treat coronavirus disease 2019 (COVID-19). *Drug Discoveries & Therapeutics* (2020) doi:10.5582/ddt.2020.01012.
61. Wu, C. *et al.* Analysis of therapeutic targets for SARS-CoV-2 and discovery of potential drugs by computational methods. *Acta Pharmaceutica Sinica B* (2020) doi:10.1016/j.apsb.2020.02.008.
62. Thanh Le, T. *et al.* The COVID-19 vaccine development landscape. *Nature reviews. Drug discovery* (2020) doi:10.1038/d41573-020-00073-5.
63. Alattar, R. *et al.* Tocilizumab for the treatment of severe coronavirus disease 2019. *Journal of Medical Virology* (2020) doi:10.1002/jmv.25964.
64. Huang, X., Pearce, R. & Zhang, Y. De novo design of protein peptides to block association of the SARS-CoV-2 spike protein with human ACE2. *Aging* (2020) doi:10.18632/aging.103416.
65. Ho, T. Y. *et al.* Design and biological activities of novel inhibitory peptides for SARS-CoV spike protein and angiotensin-converting enzyme 2 interaction. *Antiviral Research* (2006) doi:10.1016/j.antiviral.2005.10.005.
66. Vilas Boas, L. C. P., Campos, M. L., Berlanda, R. L. A., de Carvalho Neves, N. & Franco, O. L. Antiviral peptides as promising therapeutic drugs. *Cellular and Molecular Life Sciences* (2019) doi:10.1007/s00018-019-03138-w.
67. Chong, H. *et al.* A Lipopeptide HIV-1/2 Fusion Inhibitor with Highly Potent In Vitro, Ex Vivo, and In Vivo Antiviral Activity. *Journal of Virology* (2017) doi:10.1128/jvi.00288-17.
68. Lenci, E. & Trabocchi, A. Peptidomimetic toolbox for drug discovery. *Chemical Society reviews* (2020) doi:10.1039/d0cs00102c.
69. Vagner, J., Qu, H. & Hruby, V. J. Peptidomimetics, a synthetic tool of drug discovery. *Current Opinion in Chemical Biology* (2008) doi:10.1016/j.cbpa.2008.03.009.

Table

Table 1: HADDOCK docking statics of various ΔABP peptides.

Peptides	HADDOCK score*	Van der Waals energy (E_{vdw}) (kcal mol^{-1})	Electrostatic energy (E_{elec}) (kcal mol^{-1})	Desolvation energy (E_{desol}) (kcal mol^{-1})	Restraints violation energy (E_{AIR}) (kcal mol^{-1})	PRODIGY dissociation constant nM (G kcal mol^{-1})
ΔABP-α1	-68.7 +/- 5.0	-53.7 +/- 4.5	-217.4 +/- 26.4	-2.3 +/- 2.4	308.1 +/- 20.08	2.6 (-11.7)
ΔABP-α1-V10K	-71.7 +/- 8.6	-51.0 +/- 2.1	-236.7 +/- 30.2	-2.0 +/- 0.6	286.8 +/- 67.00	16.0 (ΔG -10.6)
ΔABP-α1-D25Y	-70.6 +/- 3.8	-61.5 +/- 5.0	-127.5 +/- 42.2	-16.8 +/- 3.1	331.9 +/- 72.20	5.2 (-11.3)
ΔABP-α1-V10K-D25Y	-66.0 +/- 4.9	-49.8 +/- 5.8	-161.6 +/- 31.5	-19.2 +/- 5.2	353.2 +/- 62.52	69.0 (-12.6)
ΔABP-α2	-74.0 +/- 5.3	-54.9 +/- 5.3	-200.6 +/- 15.1	-10.0 +/- 3.8	310.2 +/- 64.25	0.049(-14.1)

*HADDOCK score: 1.0 E_{vdw} + 0.2 E_{elec} + 1.0 E_{desol} + 0.1 E_{AIR}

Figures

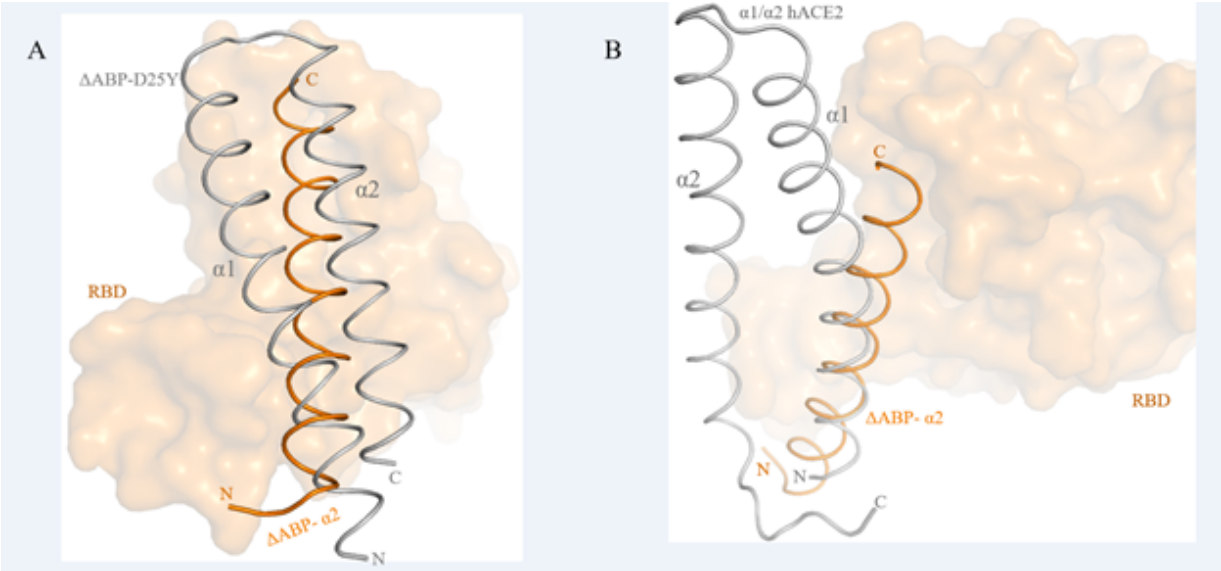

Figure 1

Binding of peptide inhibitor ΔABP-α2 on the SARS-CoV-3 RBD. A) the peptide inhibitor ΔABP-α2 binds between the two helices of ΔABP-D25Y. The receptor binding site is shown as surface. B) The Peptide

inhibitor ΔABP-α2 binding partially overlaps with the α1/hACE2. The ΔABP-α2 inhibitor showed much higher affinity for hACE2 because it forms more interaction with hACE2.

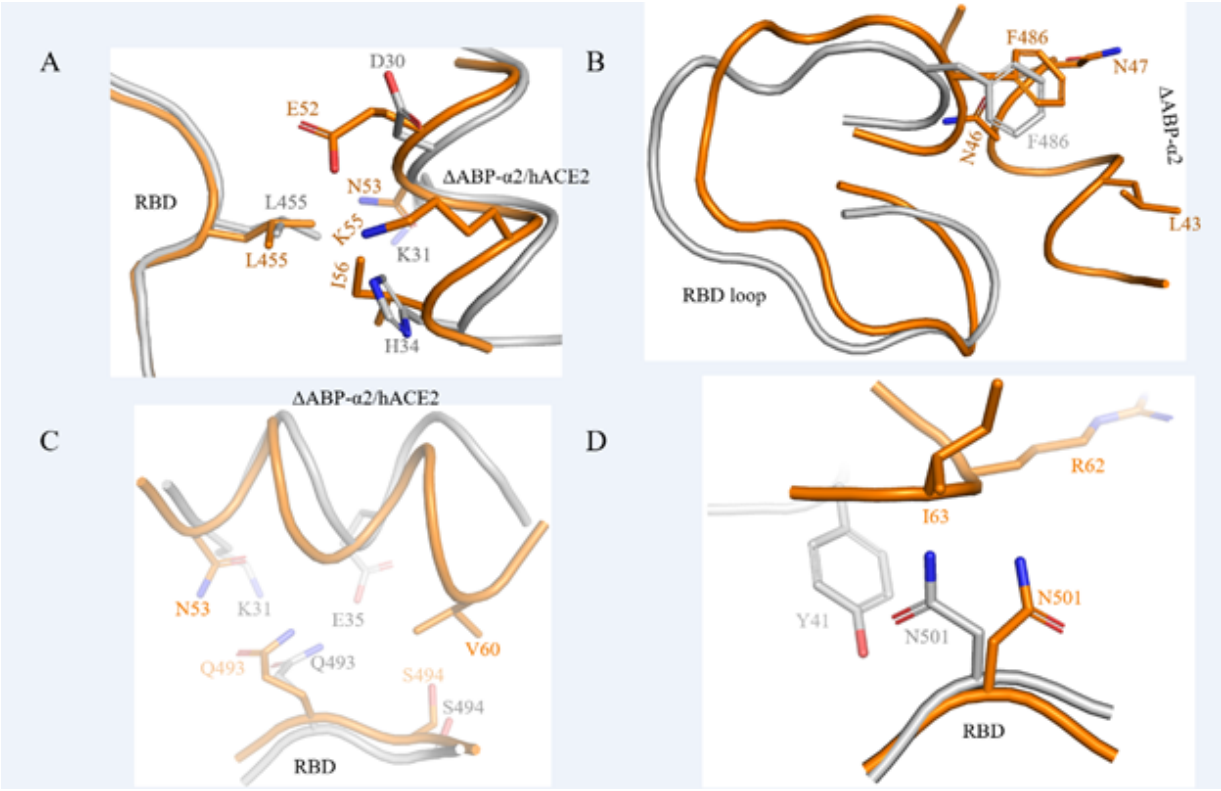

Figure 2

Interaction of viral RBD and ΔABP-α2 peptide. All critical amino acid residues A) Leu455; B) Phe486, C) Gln493, Ser494 and D) Asn501 are involved in the interaction with ΔABP-α2 peptide. SARS-CoV-2 RBD/ ΔABP-α2 complex is shown in orange and SARS-CoV-2 RBD/hACE2 complex is shown in grey.

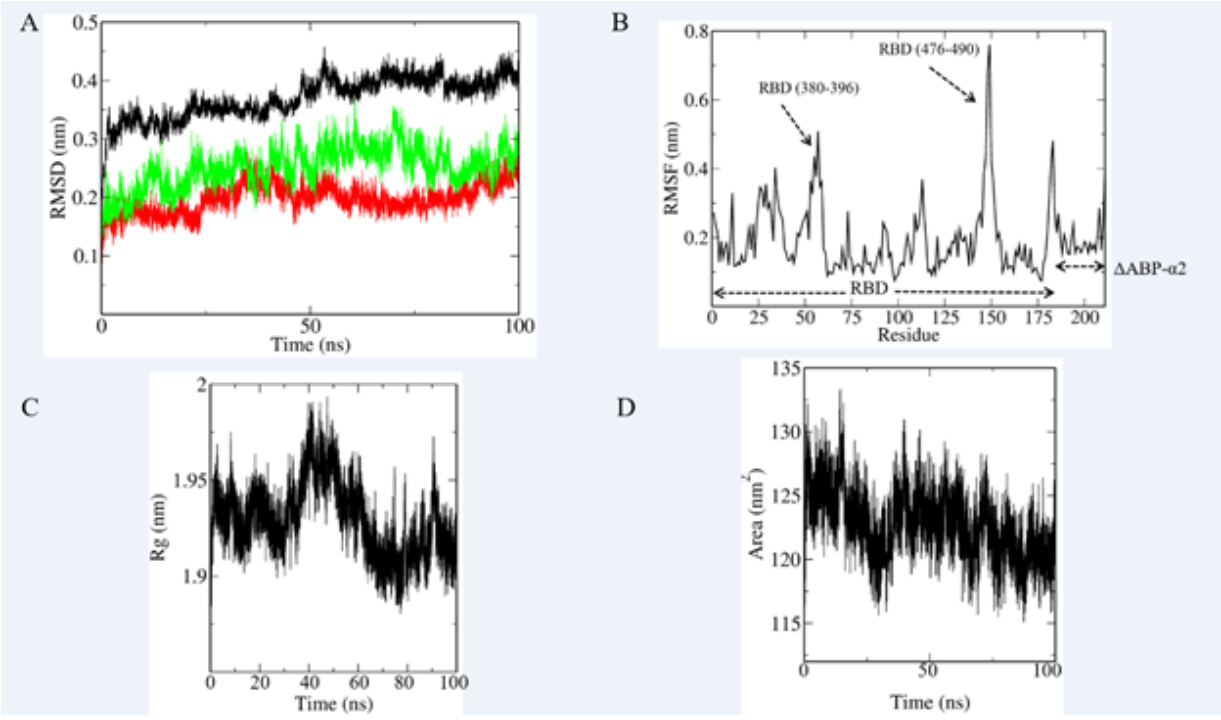

Figure 3

MD simulation of SARS-CoV-2 RBD/ΔABP-α2 complex. A) RMSD analysis of MD simulation trajectory of whole complex (black), peptide inhibitor (green) and RBM site (red). B) Averaged root-mean-square fluctuation for each amino acid in SARS-CoV-2 RBD/ΔABP-α2 complex. RBD and ΔABP-α2 peptide residues are shown by dotted arrow. C) Radius of gyration (Rg) of the complex during the 100ns simulation. D) solvent accessible surface area (SASA) is shown during simulation.

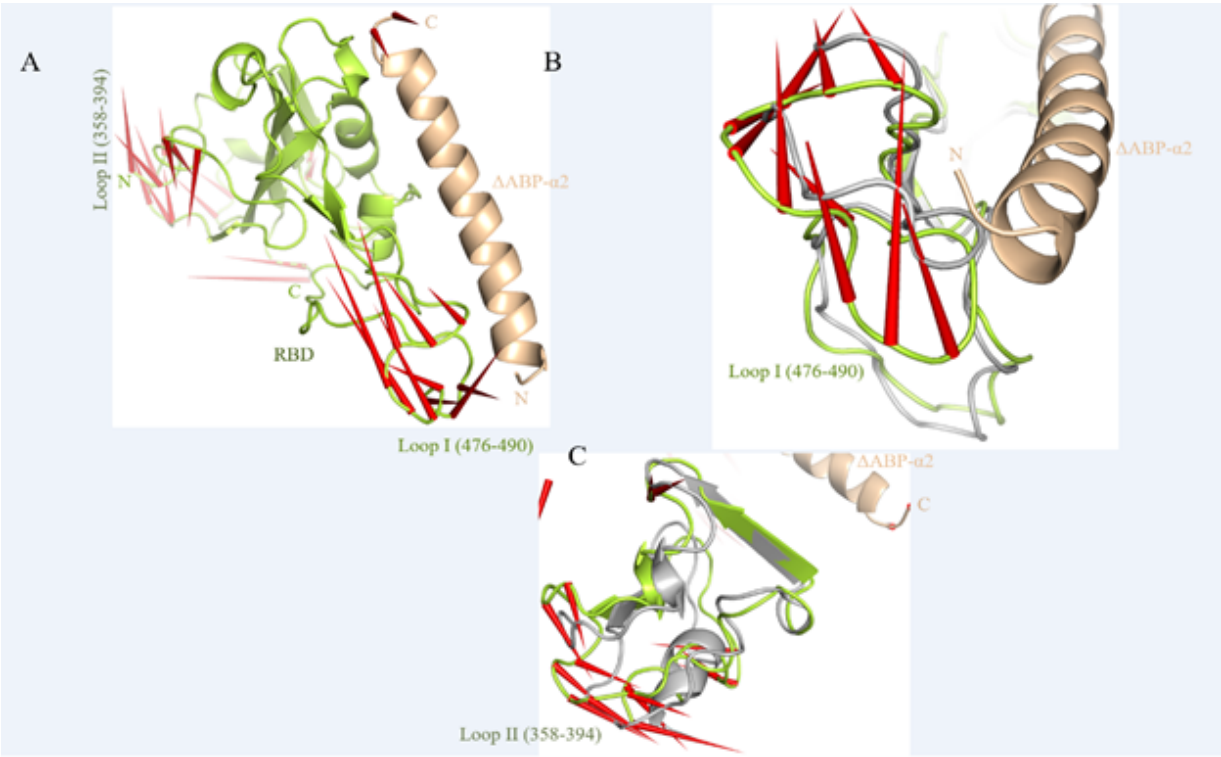

Figure 4

Dominant motion of SARS-CoV-2/ΔABP-α2 complex using principle component analysis. A) Porcupine plot of the first eigenvector of SARS-CoV-2/ΔABP-α2 complex. B) The capping loop I (476-490) near RBM site and C) loop II (358-394) shows the maximum motion. SARS-CoV-2 RBD and ΔABP-α2 are shown in limon and wheat colour. Last frame of RBD is shown in grey.

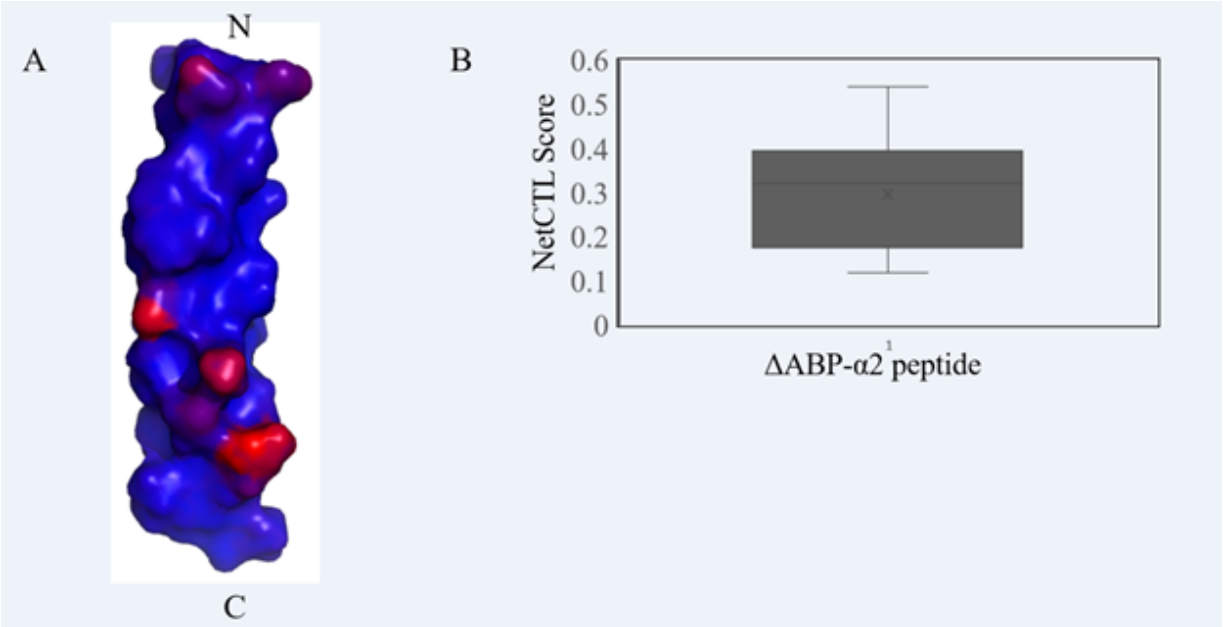

Figure 5

Immunoinformatics analysis of peptide ΔABP-α2 peptide. A) DiscoTope analysis predicted the propensity score of B cell epitope. The residues shown in red are potential B cell epitope. B) Box plot depicting NetCTL scores for predictions of cytotoxic T lymphocyte (CTL) epitopes on ΔABP-α2 peptide.

Supplementary Files

This is a list of supplementary files associated with this preprint. Click to download.

- Supp1.png
- SuppFile1.pdb
- SuppFile2.pdb